Development of Immunomodulatory Exosomal Nanocarriers to Treat Melanoma

Thomas A. Noel, M.S. and Joshua L. Hood, M.D., Ph.D.
Department of Pharmacology and Toxicology and the James Graham Brown Cancer Center,
University of Louisville School of Medicine

Introduction

Melanoma cells have been shown to communicate both locally and long range with tissues via secretion of exosomes. Exosomes are biological nanovesicles released by cells. They are analogous to non-replicating retroviruses such as HIV. Recently, we discovered that melanoma exosomes naturally home to lymph nodes and prepare them for tumor metastasis (1, 2). Tumor exosomes also can interact with and suppress anti-tumor immune cells which further facilitates metastasis (3). Similarly, pro-tumor macrophages in lymph nodes contribute to immune suppression as well. Based on their natural ability to home to lymph nodes and interact with immune cells, we believe that exosomes might be modified as immunotherapeutic nanocarriers to antagonize induction of pro-tumor macrophages.

Melittin is a 26 amino acid, alpha helical, cytolytic peptide derived from *Apis mellifera* (honeybee) venom (4). Melittin enters cell membranes as a monomer where it oligomerizes, creating pores which cause cell death (5). Recent work has shown melittin to have viral vaccine adjuvant properties (6).

Here, we aim to investigate the use melanoma exosomes as nanovesicle carriers for the immunogenic test cargo melittin. We hypothesize that melittin loaded into the membrane of exosomes should allow for the release of potentially pathogenic RNA content while keeping the exosome structure largely intact. We further hypothesize that melittin loaded into exosomes will be non-cytotoxic compared to free melittin given that the peptide's pore forming activity has been neutralized. By precisely dosing B16 exosomes with melittin, we plan to maximize melittin content while preserving exosome biophysical properties (size and zeta potential) that allow exosomes to naturally interact with macrophage cells *in vitro*. We further hypothesize that melittin modified versus unmodified melanoma exosomes will modulate macrophage inflammatory cytokine production. This will support the proof of principle that exosomes might be exogenously modified for use as immunomodulatory nanocarriers to treat melanoma.

Methods

- Cell culture – B16-F10 and RAW264.7 cells were cultured in DMEM with 10% FBS at 37 °C and 5% CO2 in 75 and 300 cm^2 flasks.
- Exosome Isolation – Exosomes were isolated from cell culture media using differential centrifugation (7). Exosome yield was quantified by protein mass using BCA (bicinchoninic acid) assay.
- Melittin Loading – Exosomes were loaded with melittin by mixing. Melittin loading was measured via UV absorbance of released RNA (8).
- Characterization of Exosome Biophysical Properties – Exosome size and zeta potential were measured using Izon qViro TRP (tunable resistive pulse) sensing.
- Cell Viability – PrestoBlue cell viability reagent was used to quantify viability of untreated cells and cells treated with free melittin, unmodified exosomes, and melittin modified exosomes
- Macrophage Inflammatory Response – cytokines in cell culture media of untreated and treated macrophages were detected using a Qiagen Multi-Analyte ELISArray.

Results

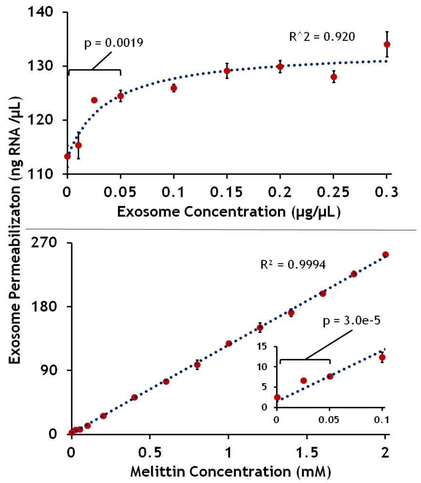

Figure 1 – Determining melittin association with melanoma exosomes through membrane permeabilization. Previously we established that exosome RNA release could be used to determine the extent of exosome permeabilization for loading cargo (8). Here we demonstrate that exosome permeabilization increases with increasing exosome concentration while keeping melittin concentration (1 mM, top) constant. Exosome permeabilization also increases with increasing free melittin concentration while keeping exosome concentration (0.05 µg/µL, bottom) constant. (n_{top}=5, n_{bottom}=4), Error bars = SEM

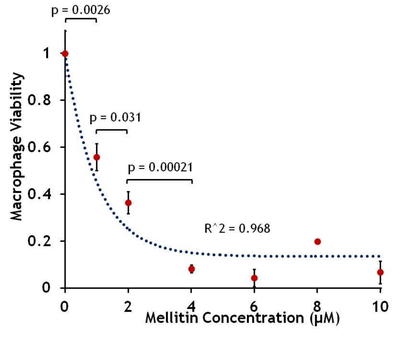

Figure 4 – Effect of free melittin on macrophage viability. Melittin is a cytolytic peptide which enters lipid bilayers, oligomerizes, and forms pores causing cell death. Here, we demonstrate that concentrations of free melittin > 2 µM are toxic to macrophages. (n=8), Error bars = SEM

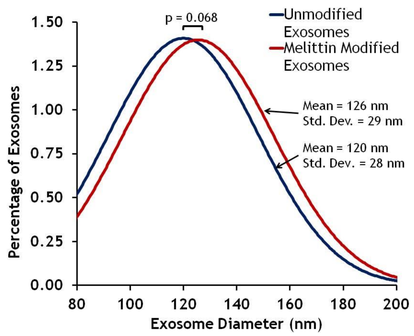

Figure 2 – Assessment of exosome size change following melittin loading. Our previous data demonstrated that melanoma exosomes naturally home to lymph nodes (1). *In vivo* trafficking properties of nanoparticles are known to be dependent on particle size. In this experiment, we sought to load exosomes with melittin while still achieving a normal exosome size distribution so as not to influence their natural trafficking properties for evaluating future *in vivo* applications. Here we demonstrate that loading B16 melanoma exosomes at a concentration of 50 µM melittin did not produce a statistically significant change in size. ($n_{unmodified}$=186, $n_{melittin}$=172)

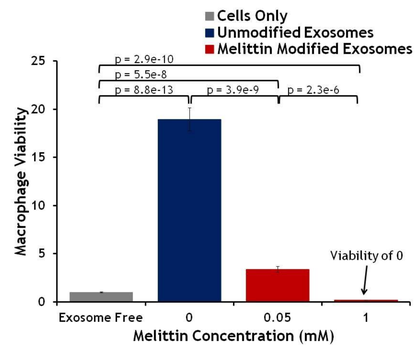

Figure 5 – Effect of unmodified and melittin modified exosomes on macrophage viability. RAW264.7 macrophages were cultured in plain media, media with unmodified B16 exosomes, and media with melittin modified B16 exosomes. Exosomes were modified at various concentrations of melittin (horizontal axis) and were added at a concentration of 0.05 µg/µL to the cells. Unmodified exosomes greatly increased macrophage activity. An equivalent amount of exosomes modified with 0.05 mM melittin increased cell activity, while those modified with 1 mM melittin caused complete cell death. This suggests a maximum level of melittin loading into exosome membranes beyond which un-neutralized free melittin collects within the intraluminal space of exosomes. (n=7), Error bars = SEM

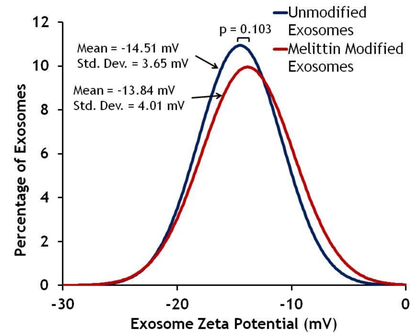

Figure 3 – Assessment of exosome zeta potential following melittin loading. In addition to nanovesicle size dictating trafficking interactions *in vivo*, particle electrokinetic mobility (zeta potential) influences particle behavior *in vivo*. Melittin is positively charged under physiological conditions. Loading too much melittin into exosome membranes would be expected to decrease their negative charge. The negative charge is physiologic to allow for natural *in vivo* circulation. Here we demonstrate that loading B16 melanoma exosomes at a concentration of 50 µM melittin did not disrupt their naturally negative zeta potential. This should serve to maintain their natural trafficking properties for testing future *in vivo* applications. ($n_{unmodified}$=186, $n_{melittin}$=172)

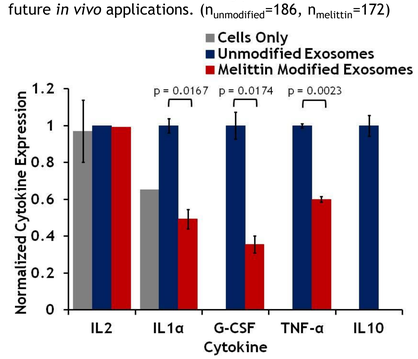

Figure 6 – Effect of unmodified and melittin modified melanoma exosomes on macrophage inflammation. Given our previous data demonstrating that equivalent amounts of both unmodified and melittin modified melanoma exosomes increased macrophage cell viability but to differing extents, we hypothesized that there might be corresponding differences in inflammatory cytokine production. These data revealed that unmodified melanoma exosomes induced greater RAW264.7 cell expression of the pro-angiogenic cytokines IL-1α and G-CSF and the immunosuppressive cytokine IL-10. IL-1α induction by melittin modified melanoma exosomes was less than non-exosome treated cells. Also, melittin modified exosomes induced no expression of the immunosuppressive cytokine IL-10. (n =2), Error bars = SEM

Conclusions

The natural ability of melanoma exosomes to home to lymph nodes and interact with immune cells makes them ideal therapeutic nanocarriers to antagonize pro-tumor inflammatory pathways. Herein, we hypothesized that the powerful immune adjuvant melittin might be stably integrated into exosomal membranes without disrupting natural exosome biophysical characteristics. Through this integration, free melittin's cytolytic toxicity would be neutralized and the exosome membrane pores formed by melittin's oligomerization would be beneficial in allowing release of internal pathogenic exosomal RNA.

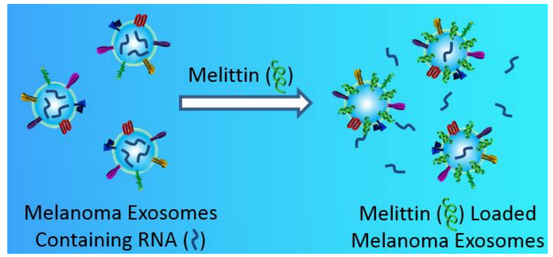

Figure 7 – A model for melittin loading of exosomes.

Our results demonstrated that melittin can be loaded into melanoma exosome membranes and form pores as evidenced by RNA release indicating membrane permeability. Loading exosomes with proper amounts of melittin allowed for this permeability without substantially altering key biophysical properties (size and zeta potential) that allow for normal *in vivo* trafficking. Melanoma exosomes modified with low concentrations of melittin (0.05 mM) also increased macrophage activity, though to a lesser degree than unmodified melanoma exosomes. Melanoma exosomes modified with high concentrations of melittin (1.0 mM) caused complete macrophage cell death. This suggests an upper limit to melittin loading capacity above which un-neutralized free melittin is likely being carried by exosomes intraluminally.

Macrophage cytokine expression profiles differed between unmodified and melittin modified melanoma exosome treatments. Melittin modified melanoma exosomes decreased the expression of pro-angiogenic IL-1α and G-CSF (7) and induced no expression of the immunosuppressive cytokine IL-10 compared to unmodified exosomes.

Collectively, these findings demonstrate the successful conversion of melanoma exosomes into non-cytotoxic melittin nanocarriers with the potential to antagonize induction of pro-tumor macrophages. Future research directions will involve further optimization of the melittin loading process. Additional *in vivo* investigations will be pursued to evaluate whether melanoma exosomes retain their innate lymph node homing ability following melittin loading and whether melittinized melanoma exosomes can antagonize macrophage pro-tumor inflammatory processes in lymph nodes. The long term goal is to develop personalized exosome based immunotherapies and vaccines for melanoma.

References

1. Hood, J.L., R.S. San, and S.A. Wickline, Exosomes released by melanoma cells prepare sentinel lymph nodes for tumor metastasis. Cancer Res, 2011. 71(11): p. 3792-801.
2. Hu, L., S.A. Wickline, and J.L. Hood, Magnetic resonance imaging of melanoma exosomes in lymph nodes. Magn Reson Med, 2014(DOI: 10.1002/mrm.25376).
3. Zhang, H.G. and W.E. Grizzle, Exosomes and cancer: a newly described pathway of immune suppression. Clin Cancer Res, 2011. 17(5): p. 959-64.
4. Soman, N.R., et al., Molecularly targeted nanocarriers deliver the cytolytic peptide melittin specifically to tumor cells in mice, reducing tumor growth. J Clin Invest, 2009. 119(9): p. 2830-42.
5. Yang, L., et al., Barrel-stave model or toroidal model? A case study on melittin pores. Biophys J, 2001. 81(3): p. 1475-85.
6. Dezfuli, H.T., et al., Induction of IFN-gamma cytokine response against hepatitis B surface antigen using melittin. Gastroenterol Hepatol Bed Bench, 2014. 7(2): p. 108-17.
7. Hood, J.L., et al., Paracrine induction of endothelium by tumor exosomes. Lab Invest, 2009. 89(11): p. 1317-28.
8. Hood, J.L., M.J. Scott, and S.A. Wickline, Maximizing exosome colloidal stability following electroporation. Anal Biochem, 2014. 448: p. 41-9.5

Acknowledgements

Research was supported by the NCI R25 grant University of Louisville Cancer Education Program NIH/NCI (R25-CA134283), the School of Medicine Summer Research Scholar Program, NIH/NIGMS (R21-GM107894) and the Elsa U. Pardee Foundation.

UNIVERSITY OF LOUISVILLE

Regulation of Oncogenic Gene Expression by Cigarette Smoke Components

Chukwuka Okafor, Melissa Metzler, Rajarshi Guha, and Douglas Darling
Departments of Oral Health and Rehabilitation
University of Louisville School of Dentistry

Introduction

Oral Squamous Cell Carcinoma (OSCC) represents more than 90 percent of all head and neck cancers. In the United States close to 46,000 Americans will be diagnosed with oral or pharyngeal cancer this year. It will cause over 8,650 deaths, killing roughly 1 person per hour, 24 hours per day. Of those 46,000 newly diagnosed individuals, only slightly more than half will be alive in 5 years. Historically the death rate associated with this cancer is particularly high not because it is hard to discover or diagnose, but due to the cancer being routinely discovered late in its development. Mouth cancer is a major neoplasm worldwide and theoretically should be largely preventable or detectable at an early stage. Epithelial to Mesenchymal Transition (EMT) is an important cellular process in growth, development, and wound healing, and drives metastasis of cancers, including OSCC.

ZEB is a transcription factor that is implicated in EMT. During the cellular process of EMT, cells undergo a morphological change and expression of mesenchymal characteristics are established. Induction of ZEB yields a suppression of E-cadherin and an upregulation of angiogenesis and chemo resistance ultimately resulting in metastasis for cells to become motile and travel to distant organ sites. In lung and gastric cancer cell lines, nicotine indirectly activates ZEB gene expression. However, this has not been investigated in oral cancer.

Hypothesis and Goal

Hypothesis: Nicotine stimulates expression of ZEB1 and ZEB2 in oral gingival cells.

Goal: Investigate the possible direct correlation in increase between Nicotine dosage and ZEB mRNA expression within human oral epithelium, using Telomerase Immortalized Gingival Keratinocytes (TIGK).

Methods

Cell Culture
TIGK cells within a cultured cell flask with DermaLife Basal Medium were allowed to cultivate to about a 90% confluence before the splitting of the cells occurred. Cells were split using Trypsin enzyme followed by an accurate counting of the cells so that each designated well had an equal value of cells per well in each plated well. Treatments of Methanol (control) and Nicotine (experimental): 400ng/mL, 600ng/mL followed for approximately 24 hours before being placed in Trizol for RNA Extraction.

RNA Isolation
Trizol reagent was utilized as an initial means in starting the RNA isolation process. The isolation of high quality RNA concentrations was measured using the NanoDrop.

cDNA Synthesis
First-strand cDNA synthesis was performed using High Capacity cDNA Reverse Transcription Kit with the DNA Engine Gradient Cycler.

RT PCR (TaqMan)
cDNA was converted to dDNA via Taqman PCR. Utilization of GADPH, ZEB1, and ZEB2 primers were incorporated in the expression assays. Data was analyzed by ΔΔCT method, where gene of interested was ZEB1 and ZEB2. Error bars represent the standard deviation of three independent experiments.

Results

1A

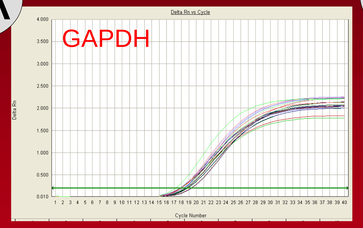

1B

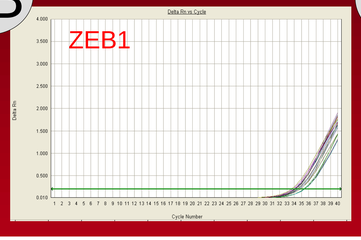

1C

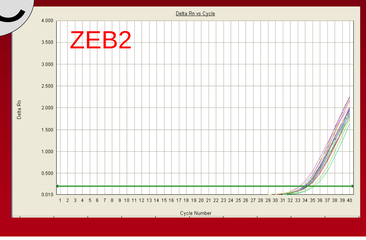

Figure 1: Results from a single TaqMan qPCR experiment. RNA from triplicate wells of nicotine-treated or control cells was converted to cDNA and assayed with probes for GAPDH (Fig 1A), ZEB 1 (Fig 1B) or ZEB 2 (Fig 1C) using Taqman primers. The figures show good quality amplification curves clearly detecting both ZEB1 and ZEB2. The relative expression patterns showed no change in the amplification curves after nicotine treatment.

2

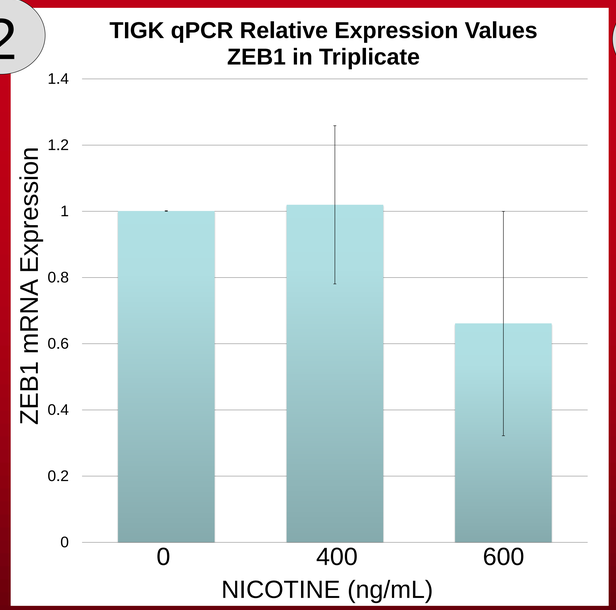

3

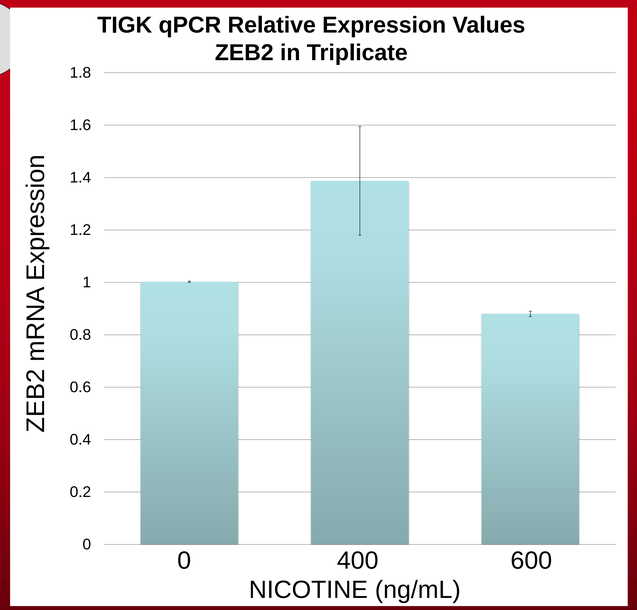

Discussion

ZEB1 and ZEB2 are protein transcription factors that are involved in metastasis of several cancers. Metastatsis is an accepted hallmark of the spread of cancer. The ZEB family of transcription factors has been implicated in cancer progression and metastasis in part due to the role it plays in EMT.

These oral gingival cells do not activate the ZEB genes in response to nicotine, which is different from the reported response of gastric and lung cells. This may be due to the cell-specific effects of nicotine, or it may be that the telomerase immortalized cells do not behave the same as normal gingival cells. Generally, nicotine exerts it biological function though the nicotinic receptor, which may be poorly expressed in this cell line.

It would be of interest to determine whether nicotine does stimulate another EMT-activating gene, such as SNAIL or Twist, in this cell line

Figure 2: TIGK qPCR Relative Expression Values of ZEB 1 in Triplicate.

Figure 3: TIGK qPCR Relative Expression Values of ZEB 2 in Triplicate.

Results graphed TaqMan qPCR relative expression of either ZEB1 or ZEB2 mRNA in TIGK cells treated with nicotine (0, 400, or 600 ng/mL). Results from 3 experiments run in triplicate are shown; error bars represent the Standard Error of Mean (SEM). Zeb1 and Zeb2 are normalized to GAPDH. Two-Sample t-test with unequal variances was conducted showing that there was no significant difference as compared to controls. With Zeb1 expression of Methanol vs Nicotine 400 ng/mL and Nicotine 600 ng/mL the two-tail results were .94 and .49 respectively. *Statistically insignificant difference*. With Zeb2 expression of Methanol vs Nicotine 400 ng/mL and Nicotine 600 ng/ml the two-tail results were .16 and .05 respectively. *Statistically insignificant difference*.

Conclusions

Though Expression Values of both ZEB 1 and ZEB 2 show inconsistencies, it is apparent that nicotine does not play a role stimulating expression of ZEBs in these cells, which may be worthy of further study to determine the detailed cell-specific mechanism(s) involved.

Acknowledgements

Research supported by a grant from University of Louisville Cancer Education Program National Cancer Institute grant R25-CA134283.

Can Cancer Cell Lines Clarify Molecular Mechanisms of Hereditary Non-Polyposis Colorectal Cancer?

Henry Roberts BS, Michael McClain BS, Jonathan Rice MD, Jane Carter MBChB, James Burton BA, Susan Galandiuk MD

Hiram C. Polk Jr. MD Department of Surgery, University of Louisville School of Medicine, Price Institute of Surgical Research and the Section of Colorectal Surgery, Louisville, KY

Introduction

- Sporadic colon cancer (CC) is commonly caused by chromosomal instability
- Hereditary non-polyposis colorectal cancer (HNPCC) is characterized by microsatellite instability (MSI)
- HNPCC is associated with different clinical manifestations and improved survival but responds poorly to 5-FU based chemotherapy compared to sporadic CC patients
- HCT116 is a widely used experimental Dukes' D CC cell line not commonly known to be derived from an HNPCC patient
- A molecular characteristic of HNPCC is inherited mutations in DNA mismatch repair (MMR) leading to MSI
- We have demonstrated different microRNA (miR) expression patterns between HCT 116 and other sporadic colon cancer cell lines with respect to miR-99a
- miR-99a an established inhibitor of mammalian Target of Rapamycin (mTOR) [Figure 1]
- Increases in mTOR protein have been shown to:
  - Increase cell growth, proliferation, migration and invasion
  - Decrease apoptosis
- miR-99a is a potential pathway for CC treatment and reducing metastasis

Figure 1: mTOR pathway

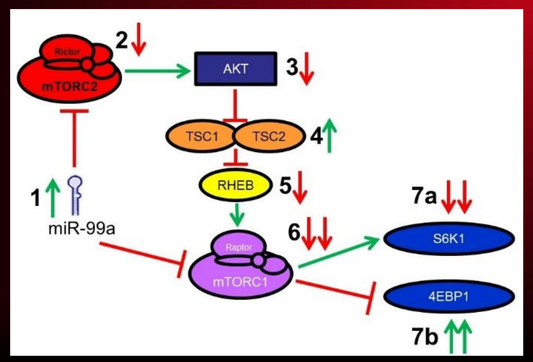

Hypothesis

We hypothesize the influence of miR-99a on the mTOR pathway, with respect to cell proliferation and motility, is dissimilar between MMR wild type (MMR+) and mutant (MMR-) CC cell lines.

Methods

All cell lines (Table 1) were transfected with miR-99a mimic (99M) and a negative control (M^-) . Transfection efficiency was verified via qPCR. mRNA and protein substrates of both mTOR complexes were analyzed by qPCR and western blot, respectively. Boyden chamber functional assays were performed measuring cell migration and invasion.

Table 1:

Cell Line	Dukes' Colon Cancer Staging	Mismatch Repair Status
HT-29	Dukes' C	Wild Type
HCT15	Dukes' C	Mutant
T84	Dukes' D	Wild type
HCT116*	Dukes' D	Mutant
CCD841	Normal Colon Epithelium	Wild Type

***Derived from a patient with HNPCC**

Results

- All cell lines were successfully transfected and showed significant upregulation of miR-99a (p<0.001)
- mRNA levels of proteins of interest were unchanged for all cell lines measured irrespective of transfection group (Figure 2)
- After transfection with 99M, total mTOR protein was decreased as compared to M- for all cell lines (Figure 3)
- Migration decreased after transfection with 99M for all cell lines as compared to M- except for the HCT116 cell line (Figure 4)
- Invasion assays showed no difference in either transfection group

Results

Figure 2:

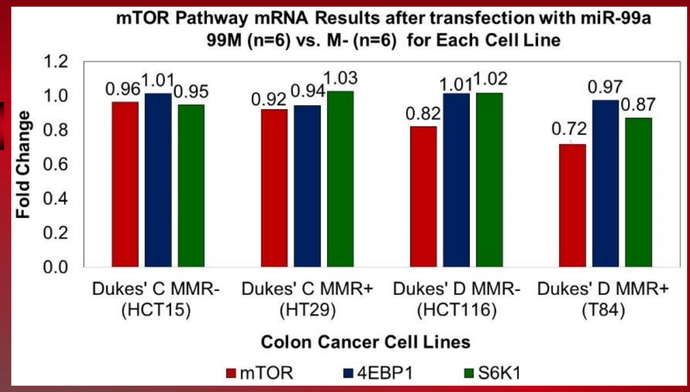

Figure 3:

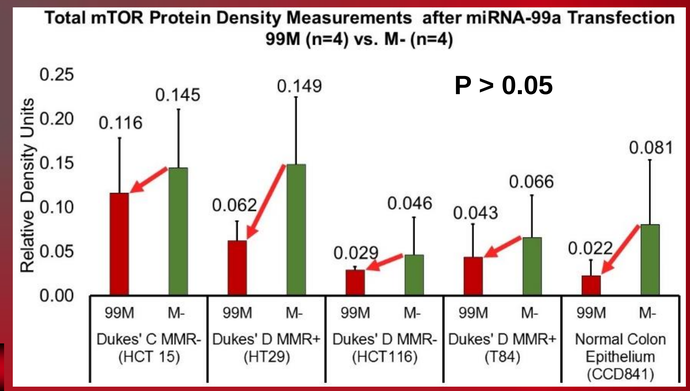

Figure 4:

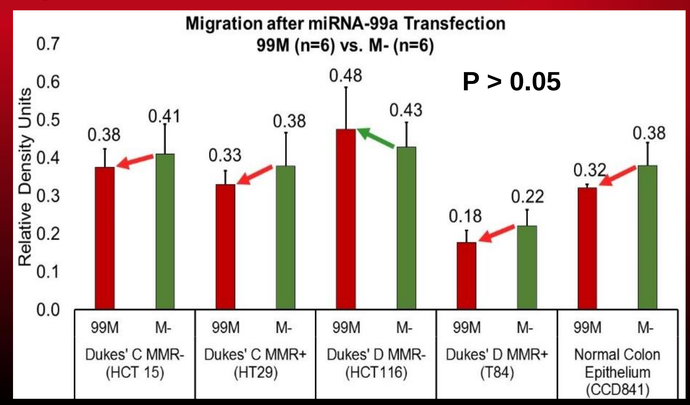

Conclusions

- Transfection of miR-99a significantly ***up-regulated*** miR-99a when compared to negative control
- mRNA expression levels for mTOR, 4EBP1 and S6K1 were ***unchanged*** after transfection with miR-99a when compared to negative control
- Total mTOR was ***decreased*** in Dukes' C MMR-, Dukes' C MMR+, Dukes D MMR+ CC cell line after transfection with miR-99a compared to negative control
- Migration ***decreased*** after transfection with 99M for all cell lines as compared to M- except for the Dukes' D MMR+ cell line
- Invasion assays showed ***no difference*** in either transfection group
- We believe these results show a promising difference in the molecular mechanism regulating the mTOR pathway between HNPCC compared to sporadic colon cancer
- We intend to investigate further to identify different pathways involved in HNPCC cancers that may permit development of improved adjuvant therapy for MMR deficient cancer patients with advanced disease

Acknowledgments

National Cancer Institute grant R25-CA134283 as well as John W. and Barbara Thruston Atwood Price Family Trust

Development of a plasma miRNA panel in detecting response to treatment of colorectal adenoma and colorectal cancer

Vanessa States BS[1] , Jane Carter MBChB[1], Shesh Rai PhD[2], Jianmin Pan PhD[2], Robert Eichenberger MMS[1], Susan Galandiuk MD[1]

[1]Hiram C. Polk Jr. MD Department of Surgery, University of Louisville School of Medicine, Price Institute of Surgical Research and the Section of Colorectal Surgery, Louisville, KY

[2]Department of Bioinformatics and Biostatistics, University of Louisville School of Public Health & Information Sciences, Louisville, KY

Introduction

- Colorectal adenomas (CRA) develop into sporadic colorectal cancer (CRC) via
  - mutational activation of oncogenes
  - inactivation of tumor suppressor genes
- Carcinoembryonic antigen (CEA) is a widely used as a non-invasive plasma test used to screen for recurrent disease. Current limitations include a
  - less than optimum sensitivity and specificity
  - need for a more accurate noninvasive biomarker
- miRNAs are heavily investigated potential biomarkers for a variety of human cancers
  - stable and dysregulated in disease states.

Hypothesis

We hypothesize that microRNAs are differentially expressed in colorectal adenomas and cancer before as compared to after treatment.

Methods

Plasma was isolated from 5 patients with advanced CRA(>0.6 cm diameter +/or villous component) and 5 patients with stage II or III CRC prior to treatment and 4-6 weeks following surgical or endoscopic treatment. RNA was extracted & 768 miRNA screened using TLDA (Taqman low density array) cards. Data were analyzed using paired t-tests after normalizing raw cycle threshold data to endogenous RNU6.

Study Design

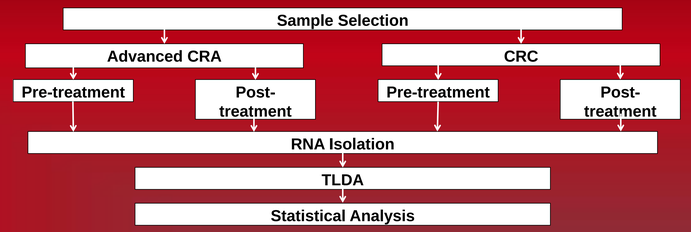

Results

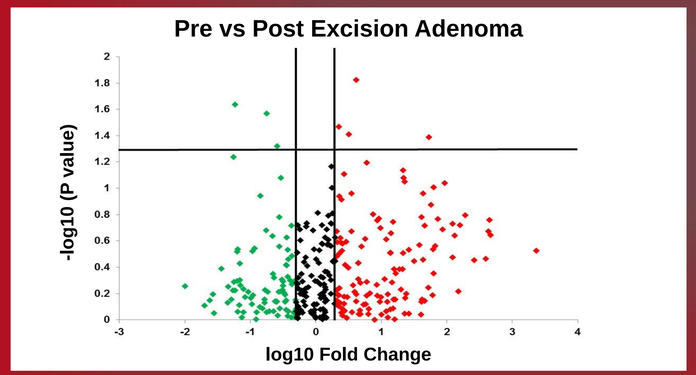

Figure 1. Comparison of microRNA expression between pre and post treatment CRA samples. Most significantly upregulated were miR-623, miR-186and miR-299-5p.

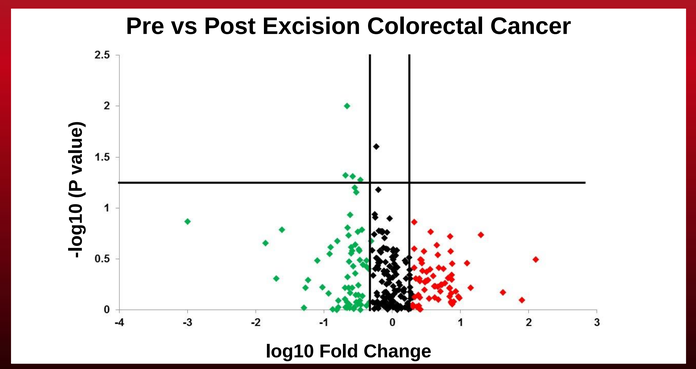

Figure 2. Comparison of microRNA expression between pre and post excision CRC samples. Most significantly downregulated were miR-766, miR-324, and miR-30d.

Results

Pre vs Post Excision Adenoma

miRNA	Fold Change	P Value
miR-623	4.149	0.015
miR-186	3.163	0.039
miR-299-5p	52.8	0.041

Pre vs Post Excision Colorectal Cancer

miRNA	Fold Change	P Value
miR-766	0.153	<0.001
miR-324	0.216	0.01
miR-30d	0.264	0.049

Figure 3. Significant microRNAs identified for pre vs post excision CRA and CRC.

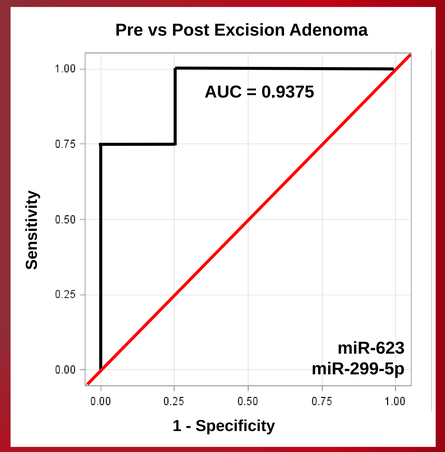

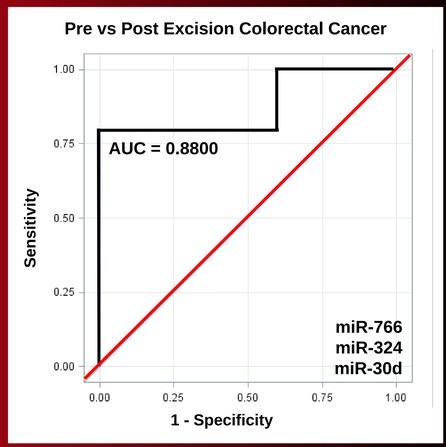

Figure 4. ROC curves for pre vs post excision CRA and CRC.

Conclusions and Future Directions

Our data suggest differences in pre and post treatment miRNA expression between in both colorectal adenomas and colorectal cancer. Further validation is needed in order to develop a diagnostic miRNA panel to monitor patients for the presence of recurrent disease.

Acknowledgments

National Cancer Institute grant R25-CA134283, John Williamson and Barbara Thruston Atwood Price Family Trust

The Role of DAB2IP in RASSF-mediated Tumor Suppression

Desmond R. Stewart[1,3], M. Lee Schmidt[1,2], and Geoffrey J. Clark[1,3]

[1]Molecular Targets Group, James Graham Brown Cancer Center, Departments of [2]Biochemistry & Molecular Biology and [3]Pharmacology & Toxicology
School of Medicine, University of Louisville, Louisville, KY, USA

INTRODUCTION

The Ras oncogene is the most notorious mediator of human cancer, with mutations found in up to 30% of screened tumors. Current literature thoroughly describes Ras' ability to induce cellular transformation through multiple signaling pathways when not appropriately regulated by its GTPase Activating Proteins (GAPs) and Guanine nucleotide Exchange Factors (GEFs). Ras also has the paradoxical ability to induce cell cycle arrest and apoptosis; however, the mechanism by which this occurs has not been fully characterized. In part, Ras appears to activate these growth suppression mechanisms via its effector, NORE1A, which is a member of the RASSF family of tumor suppressors. Ras binds NORE1A directly to promote senescence and expression of NORE1A is frequently lost in human tumors, thus facilitating Ras transformation. Unfortunately, the mechanism of action remains unclear. We have identified a tumor suppressor called DAB2IP as a direct binding partner of NORE1A. DAB2IP is frequently inactivated in human prostate cancer, and a study using knockout mice has shown that DAB2IP inactivation is sufficient for prostate adenocarcinoma development. This study implicated loss of DAB2IP-mediated suppression of NF-κB as the driver of epithelial to mesenchymal transition (EMT) and tumor metastasis. However, DAB2IP is also a negative regulator of Ras. Therefore, a NORE1A/DAB2IP interaction could modulate NF-κB and establish a feed-back loop to modulate Ras. Here we show that NORE1A and DAB2IP do indeed form a novel Ras-regulated protein complex. Furthermore, NORE1A and DAB2IP cooperate to potently activate oncogene-induced senescence (OIS), which is a key protection mechanism against hyperactive Ras signaling. Thus, loss of NORE1A and/or DAB2IP impairs the ability of the cell to protect itself against oncogenic Ras mutations, thus removing a key tumor suppressive mechanism.

METHODS

Cell Lines: HEK293T, COS7, and A549 cells were maintained in DMEM supplemented with 10% fetal bovine serum (FBS) and 1% penicillin-streptomycin. H1299 cells were maintained in RPMI supplemented with 10% FBS and 1% penicillin-streptomycin.

Fluorescence Imaging: Images were captured using a Spot 1.5.0 Camera (Diagnostic Instruments).

Co-immunoprecipitation: Cells were transfected with expression constructs tagged with either fluorescent protein (GFP or KATE) or human influenza hemagglutinin (HA) and lysed. Lysates were then incubated overnight in GFP-nAb agarose resin (Allele Biotechnology) or A2095 Monoclonal Anti-HA-Agarose (Sigma-Aldrich). Resin was washed in NP-40 lysis buffer and boiled for Western Blot analysis.

Western Blotting: Lysates were separated 4-12% Tris-Glycine gels (Invitrogen) and transferred to 0.2 um nitrocellulose membranes. After antibody incubation, protein was visualized using SuperSignal WestPico Chemiluminescent substrate (ThermoScientific)

Senescence Assay: Cells were fixed and stained for beta-galactosidase activity using the BioVision Senescence Detection Kit.

RESULTS

1

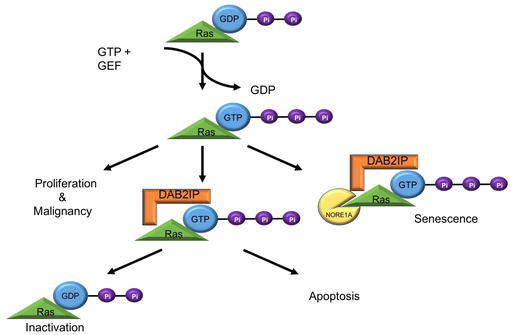

Figure 1: Schematic of proposed DAB2IP/NORE1A senescent pathway. Under the influence of a GEF, Ras exchanges GDP for GTP at the inner cellular membrane, leading to proliferation via activation of the MAPK pathway. DAB2IP binds Ras directly, activating its GTPase domain, shutting down Ras signaling. When Ras is mutated to become constitutively activated (as is the case in human tumors), the DAB2IP-Ras interaction induces apoptosis to prevent tumor development. Ras activity can be modulated by its effector proteins such as NORE1A to induce senescence.

2

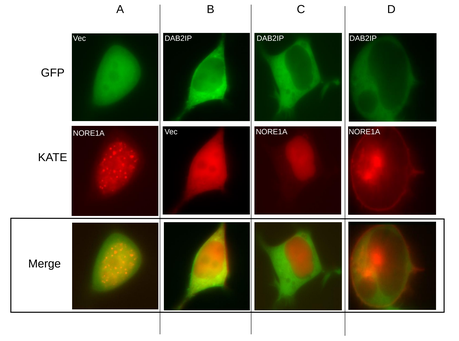

Figure 2: NORE1A and DAB2IP colocalize at the cellular membrane in the presence of activated Ras. COS7 cells were cotransfected with KATE vector and GFP-tagged DAB2IP (A), GFP vector and KATE-tagged NORE1A(B), or GFP-DAB2IP and NORE1Ain the absence (C) or presence (D) of activated H-Ras. When Ras is activated, both NORE1A and DAB2IP localize to the cell membrane.

3

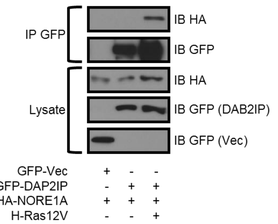

Figure 3: NORE1A forms a Ras-dependent complex with DAB2IP. HEK293T cells were transfected with expression constructs for NORE1A, DAB2IP, and activated HRas (12V). After a 48-hour incubation, cells were lysed and immunoprecipitated. NORE1A only co-localizes and precipitates when HRas is activated in the cell.

4

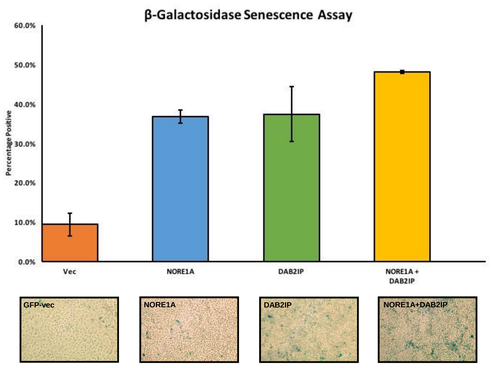

Figure 4: NORE1A and DAB2IP act to induce senescence in cancer cells. Current evidence suggests that DAB2IP promotes apoptosis of tumor cells; however, DAB2IP has not yet been shown to induce senescence. A549 cells were transfected with expression constructs for NORE1A and DAB2IP. After a 48-hour incubation. Cells were fixed and stained to detect β-galactosidase activity using the BioVision Senescence Detection Kit. Number of senescent cells counted at 10x magnification and presented as average percentage of senescent cells per field.

DISCUSSION

Both NORE1A and DAB2IP have been characterized as tumor suppressors, but their mechanisms of action are not yet fully understood. NORE1A binds Ras directly and has been shown to be a pro-apoptotic/pro-senescent Ras effector; there are multiple signaling pathways through which this may occur. NORE1A is frequently inactivated in human tumors and loss of NORE1A expression has been implicated in a hereditary cancer syndrome, further supporting its physiological role in tumor suppression. DAB2IP is a RasGAP, acting to shut down Ras signaling when under normal regulation. DAB2IP is also considered a pro-apoptotic tumor suppressor, which appears to be only partly explained by the activity of its RasGAP domain. Here we demonstrate a novel growth-suppressive role for DAB2IP as a senescence effector. Additionally, we describe a novel, Ras-regulated interaction between DAB2IP and NORE1A through fluorescence imaging and co-immunoprecipitation. Overexpression of both proteins in HEK293T cells shows us that, in the absence of Ras, DAB2IP is in the cytoplasm while NORE1A is in the nucleus. Upon addition of activated Ras, colocalization can be found strongly on the membrane (Figure 2) and complex formation was supported by immunoprecipitation experiments (Figure 3). In A549 cells containing wild-type p53 and activated Ras, overexpression of NORE1A and DAB2IP individually induced senescence; furthermore, an enhanced effect is observed when both are expressed in the same cell (Figure 4). Other defined roles for DAB2IP tumor suppression are centered around suppression of NFkB signaling. Our preliminary experiments show that NORE1A can also have a similar effect. Thus, DAB2IP may require NORE1A to suppress NFkB and this effect may be enhanced in the presence of Ras as part of a protective growth-suppressive mechanism against hyperactive growth stimulation and indeed warrants further study.

Acknowledgments

Research funding was provided by National Cancer Institute grant R25-CA134283.

Paraoxonase-2 mediates a homoserine lactone-induced apoptosis in breast cancer cells

Nicole S. Stivers, M.S.[1], Aaron G. Whitt, B.S.[1], Aaron M. Neely, M.S.[1], Guoping Zhao, Ph.D.[1], Chi Li, Ph.D.[1]

[1]Departments of Medicine, Pharmacology and Toxicology, Molecular Targets Program, James Graham Brown Cancer Center, University of Louisville School of Medicine

Abstract

Paraoxonase-2 (PON2) is an enzyme involved in the hydrolysis of organophosphates and lactones. PON2 has been reported to be over-expressed in multiple cancers, and to contribute to the resistance of conventional chemotherapeutic drugs. Our recent study found that N-(3-oxododecanoyl)-L-homoserine lactone (C12) from the bacterium *Pseudomonas aeruginosa* induced apoptosis in cancer cells dependent on PON2. However, the detailed molecular mechanism of PON2 in C12-induced apoptosis in breast cancer was unknown. In this study, we first screened a panel of human breast tissues for PON2 expression from patients with conditions ranging from normal to malignant. It was found that higher levels of PON2 were expressed in breast tissues from patients with malignant forms of breast cancer. Furthermore, upon stably reducing PON2 expression in T47-D and MDA-MB-231 breast cancer cells, significantly less cell death and caspase-3/7 activation was observed, and less release of cytochrome c was observed in T47-D cells following C12-treatment. Overall, our results demonstrate that PON2 plays a vital role in C12-induced apoptosis in breast cancer cells, which indicates PON2 might be a new target for breast cancer therapy.

Results

1. PON2 expression is elevated in human malignant breast conditions.

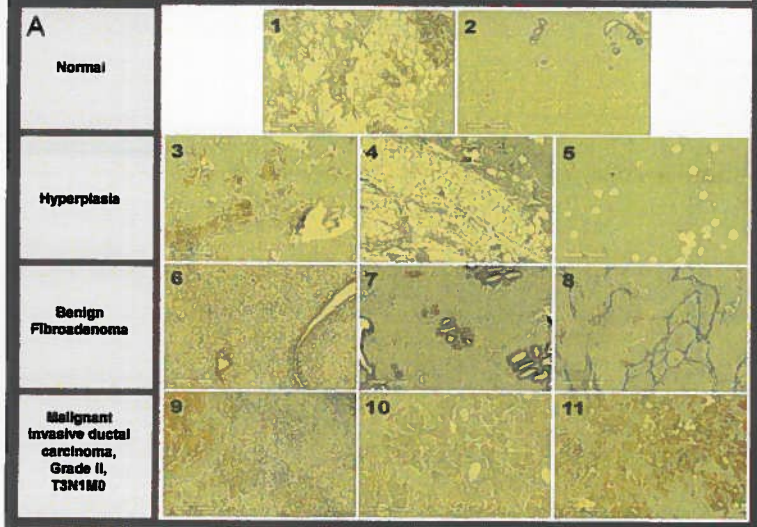

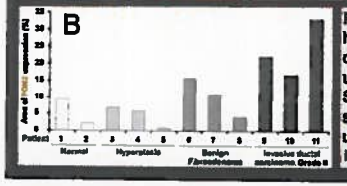

Figure 1: (A) A breast tissue array with normal (1-2), hyperplastic (3-5), benign (6-8), and malignant (9-11) conditions was screened for the expression of PON2 using a DAB with Hematoxylin counter-stain protocol. Scale bar is 300μm. (B) % Area of PON2 for each section of tissue was analyzed with Fiji(Is just ImageJ) using threshold pixel density analysis following DAB-Hematoxylin color deconvolution. (n=1)

2. PON2 is essential for C12-induced apoptosis in breast cancer cells.

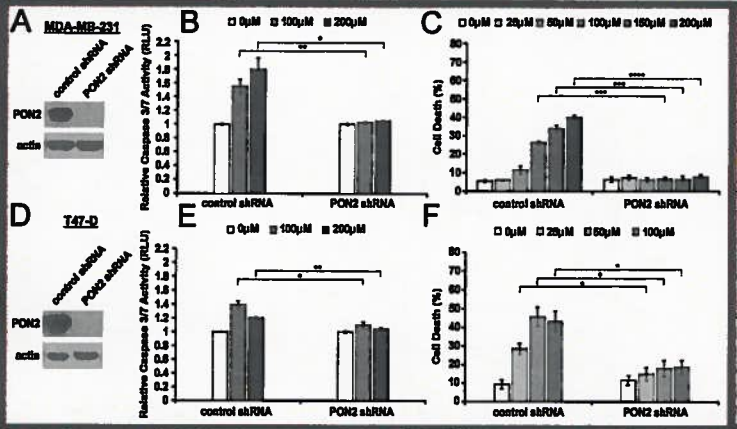

Figure 2: (A-F) Following stable reduction of PON2 expression in MDA-MB-231 (A-C) and T47-D (D-F) breast cancer cells, protein levels (A,D), relative caspase-3/7 activity following 4h C12-treatment (B,E), and percentage of PI positive cells following 24h C12-treatment (C,F) were investigated. Average ± SEM. (n=3) Student T test *, $p < 0.05$; **, $p < 0.01$; ***, $p < 0.001$; ****, $p < 0.0001$. control shRNA vs PON2 shRNA.

3. PON2 is vital for C12-induced cytochrome c release from mitochondria.

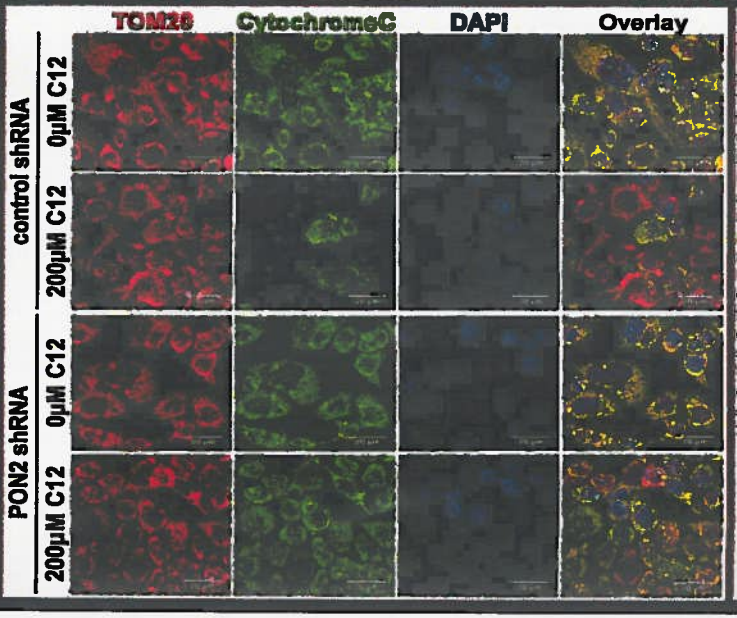

Figure 3: Control and PON2 shRNA T47-D breast cancer cells were treated with either vehicle (DMSO) or C12 for 4h. Representative confocal maximum intensity projection (MIP) images are shown. Mitochondrial marker TOM20 (red), cytochrome c (green), and DAPI (blue). Notice C12 induces less cytochrome c release from PON2 shRNA cells compared to control shRNA cells. Cytochrome c release is evident by more diffuse staining. Scale bar is 20μm.

4. PON2 is not involved in Doxorubicin-induced cell death.

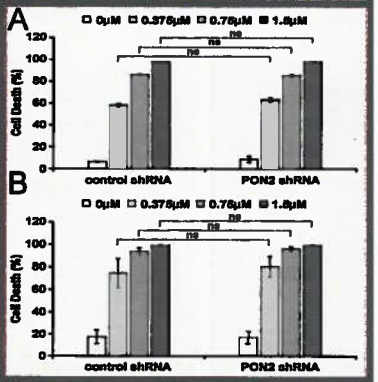

Figure 4: (A-B) Control and PON2 shRNA MDA-MB-231 (A) or T47-D (B) breast cancer cells were treated with various concentrations of Doxorubicin for 48h. Percentage of PI positive cells is shown. Average ± SEM. (n=3) Student T test. ns, not significant.

Conclusions

- PON2, which normally serves a protective function for cells from death, is ironically essential for C12-induced apoptosis.
- PON2 expression may be elevated in human breast malignant conditions compared to normal conditions, which would thereby contribute to the selectivity of C12 for breast cancer cells.
- This unique PON2-dependence of C12 offers much promise for PON2 as a new target for breast cancer therapy.
- We propose the lactonase activity of PON2 is responsible for cleavage of C12 into an active product. Further experiments have been planned to test this hypothesis.
- We also plan to expand the human breast tissue array and test our hypothesis in vivo.

Acknowledgements

This research was supported by grant R25-CA134283 from the National Cancer Institute.

UNIVERSITY OF LOUISVILLE